

Polarization choices in exciton-biexciton system of GaAs quantum wells

S. Adachi,* T. Miyashita, S. Takeyama, and Y. Takagi

Department of Material Science, Faculty of Science, Himeji Institute of Technology, 1479-1 Kamigori, Harima Science Garden City, Hyogo 678-12, Japan

A. Tackeuchi

Fujitsu Laboratories Ltd., Morinosato-Wakamiya, Atsugi, Kanagawa 243-01, Japan

M. Nakayama

Department of Applied Physics, Faculty of Engineering, Osaka City University, Sugimoto, Sumiyoshi-ku, Osaka 558, Japan

(Received 1 August 1996; revised manuscript received 20 September 1996)

We study the induced absorption due to biexciton formation in absorption bleaching pump-probe signals and the quantum beats between exciton and biexciton in the four-wave-mixing signals. The origin is confirmed by the polarization dependence of the signals in both experiments. The definite discrimination between exciton-biexciton quantum beats and the others by the polarization choices is demonstrated clearly. We also show the well-width dependence of the biexciton binding energy that is determined by the period of the quantum beats in the range of well width 45–150 Å of GaAs/Al_xGa_{1-x}As ($x=0.3-1.0$) multiple quantum wells. [S0163-1829(97)00104-5]

I. INTRODUCTION

Excitons essentially dominate the linear and nonlinear optical properties of GaAs quantum wells (QW's) near the band edge, but stabilize easily into biexcitons in the resonant excitation.^{1,2} In the range probed by ultrafast spectroscopy using femtosecond pulse lasers, the intense excitation condition is easily achieved. As a result, it is much more likely to observe the *modified* exciton dynamics by the biexcitonic contributions.³⁻⁵ In fact, recent studies of the exciton dynamics have shown that nonlinear interaction in QW's could not be described by a simple assembly of two-level systems because the exciton-exciton interaction⁶ and exciton-biexciton interaction⁷ should be taken into account.

Biexcitons have been studied in various semiconductor materials and in heterostructures. In bulk crystals, for example, Si and CuCl, the creation of biexcitons is clearly demonstrated. Theoretical work⁸ predicts a significant enhancement of the biexciton binding energy in quasi-two-dimensional systems. For GaAs QW's, several experimental works related to biexcitons^{1-4,6,7,9-19} have been published and established the existence of biexcitons. Most of these experimental studies indicate that the biexciton binding energy is 1–2 meV, which is about one order of magnitude larger than that in bulk GaAs and confirms the theoretical prediction in a sense, but its well-width dependence needs continued investigation.

The binding energy of quantum-well biexcitons in the measurement by Miller *et al.*⁹ agrees with the calculation by Kleinman⁸ for the well thickness below ~ 150 Å. But the observed binding energies for thicker QW's do not agree with the theoretical result and recent experimental studies also indicate a larger binding energy. An explanation for the discrepancy between theory and experiment has not been given yet. Recently, Birkedal *et al.*²⁰ performed a systematic experimental study of the well-width dependence of biexciton

binding energy for a range of well thickness 80–160 Å. In most of the previous works the biexciton binding energy is deduced from the energy separation of the doublet structure in the photoluminescence (PL) spectrum or the period of the quantum beat on the basis of a superlinear power dependence of the lower-energy peak in the PL spectrum.

On the other hand, Osborne *et al.*²¹ warn strongly that the lower-energy peak of the doublet structure in the low-temperature PL tends to be easily assigned to the biexciton origin. They observed strikingly similar features to the biexcitonic PL in the cw PL spectra of GaAs/Al_{0.33}Ga_{0.67}As multiple quantum wells (MQW's), such as a tailed component in the lower energy of the doublet structure, a superlinear growth of the peak against laser intensity, a binding energy of 1–2 meV, and a well-width dependence. The origin of the lower-energy PL component is attributed not to biexcitons but to positively charged excitons that are excitons bound to holes in the QW originating from the background concentration of acceptors in Al_xGa_{1-x}As barriers. They also emphasize that the superlinear power dependence in the PL spectra is not necessarily indicative of biexciton formation, as argued in previous works,^{2,3,9} because the positive-charged exciton shows the same power dependence as that of biexciton. Therefore, we require a definite discrimination between biexcitons and, for example, charged excitons or excitons bound to some localized states.

In the present work we observe the quantum beats between exciton and biexciton states and the induced absorption due to biexciton formation, respectively, in the four-wave-mixing (FWM) and pump-probe nonlinear transmission-reflection measurements in GaAs MQW's. The pump-probe technique is used for the confirmation of the biexciton formation and the polarization selection rule. The definite discrimination between biexcitons and other excitons by the FWM measurement is demonstrated on the basis of the polarization selection rule. Finally, we show the well-

TABLE I. GaAs/Al_xGa_{1-x}As QW samples investigated in the present work.

Sample	L_w (Å)	L_b (Å)	N	x	hh- e (eV)	lh- e (eV)	E_b^x (meV)
1	150	150	20	1.0	1.5370	1.5454	9.6
2	100	100	30	1.0	1.5671	1.5843	11.6
3	68	198	25	0.3	1.5804	1.6050	11.0
4 ^a	45	40	120	0.51	1.6554	1.6887	13.9

^aThe GaAs substrate was removed.

width dependence of the biexciton binding energy, determined by a period of quantum beats between the exciton and biexciton in the range of well width 45–150 Å of GaAs/Al_xGa_{1-x}As ($x=0.3-1.0$) MQW's.

II. EXPERIMENT

A. Sample and experimental setup

The samples investigated in the present work are four GaAs/Al_xGa_{1-x}As ($x=0.3-1.0$) crystals with a well width of 150, 100, 68, and 45 Å, respectively. Each sample was grown on a (001) GaAs substrate by molecular-beam epitaxy. The substrate of the sample with the 45 Å well width was removed by selective etching for various transmission-type spectroscopies. The optical properties of the other samples are measurable in the reflection geometry due to very high reflectivity. The properties of the samples are listed in Table I, where L_w , L_b , x , N , hh- e , lh- e , and E_b^x are the well width, the barrier width, the Al concentration of barrier layer, the number of pairs of well and barrier layers, the heavy-hole (hh) and light-hole (lh) exciton transition energies, and the hh exciton binding energy, respectively. The hh and lh exciton transition energies were determined from the photoluminescence excitation and absorption spectra. The exciton binding energy of each sample was calculated by the accurate theory.²²

We performed the pump-probe nonlinear transmission-reflection experiments and the FWM experiments in a two-pulse self-diffraction configuration. Depending on the sample, the reflection and/or transmission geometries were employed. A self-mode-locked titanium-doped:sapphire laser with a pulse repetition rate 76 MHz was used as a light source. The laser light with a typical pulse width at half maximum (FWHM) of 150 fs was divided into two beams, pump and probe, and the pump pulse passed through a stepping motor-driven optical delay line. The pump and probe beams with wave vector \mathbf{k}_1 and \mathbf{k}_2 were superimposed on the sample surface at an angle 6°. The relative time delay between both pulses was defined as positive (negative) in the time region where the pump pulse arrived earlier (later) than the probe pulse at the sample, and the time origin was ascertained by the measurement of second-harmonic generation from a 0.1-mm-thick potassium dihydrogen phosphate crystal at the sample position. A half-wave plate inserted into the pump beam path and a quarter-wave plate inserted into both beam paths were properly rotated to convert the linear polarization to either left or right circular polarization with a polarization extinction ratio better than 300:1 without changing the pulse intensities. The pump and probe beams were chopped with the different frequencies and the transmitted

(reflected) probe signal in the direction of \mathbf{k}_2 or the self-diffracted FWM signal in the direction of $2\mathbf{k}_2 - \mathbf{k}_1$ that modulated with the sum frequency was detected to be time integrated by a lock-in amplifier. The estimated exciton density was $\sim 5 \times 10^9 \text{ cm}^{-2}$ in our experiments. The sample was held at 10 K in a helium-flow cryostat. The probe intensity was reduced to typically one-tenth of the pump intensity in the pump-probe nonlinear transmission-reflection measurements and was adjusted to the pump pulse intensity in the FWM measurements.

B. Choice of light polarizations

The quantum confinement lifts the degeneracy between the hh and lh in the valence band at the Γ point ($\mathbf{k} = \mathbf{0}$). The lowest-energy lh subband located 8.4-33 meV above the hh subband in our samples is not resonant with the photoexcitation. For simplicity we restrict the discussion to the hh exciton. The lift of degeneracy provides a quantization axis of the exciton transition so that only transitions with $\Delta J_z = \pm 1$ are dipole allowed for the propagating pulses normal to the plane of the QW and thus the eigenpolarizations are circular, denoted by σ_{\pm} . The hh exciton is modeled in the frame of a two-level system with an angular momentum J of 3/2 and 1/2 for the lower and upper levels, respectively, which belong to the valence and conduction bands. The electron and hole that are created by resonant photoexcitation couple as an exciton by Coulomb interaction within 200 fs and we can also consider the system in the exciton picture as shown in Fig. 1.

Figures 1(a), 1(b), and 1(c) show the linkage diagrams for hh exciton and hh biexciton states in the GaAs/Al_xGa_{1-x}As QW by the optical excitation in the specific

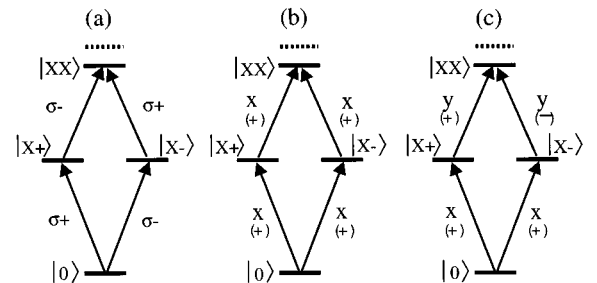


FIG. 1. Linkage diagram of the exciton-biexciton system in GaAs/Al_xGa_{1-x}As QW's. All diagrams are depicted in a helicity basis for (a) same- and opposite-circular polarizations, (b) parallel polarizations, and (c) cross-linear polarizations. The positive (+) and negative (-) signs represent the relative phases between the probability amplitudes of the transitions.

light polarizations of the pump and probe pulses. Figure 1(a) is for the same-circular and opposite-circular polarizations, Fig. 1(b) for parallel linear polarizations, and Fig. 1(c) for cross-linear polarizations.

In Fig. 1(a), the excitation by σ_+ and σ_- polarized lights can generate the exciton states $|X_+\rangle$ and $|X_-\rangle$, with angular momenta of $+1$ and -1 , respectively, from the zero angular momentum vacuum ground state $|O\rangle$. Such a three-state atom analogy in the GaAs QW is frequently used in the analysis of optical phenomena of excitons.^{6,17} The optical transition to the lowest-energy biexciton state $|XX\rangle$ can be achieved only by the excitation by σ_+ and σ_- polarized lights form $|X_-\rangle$ and $|X_+\rangle$, respectively, according to the selection rule because the uppermost state has zero angular momentum. In the figure, a two-hh exciton state is indicated by a dashed line and the energy separation between the two-hh exciton state and $|XX\rangle$ corresponds to the biexciton binding energy.

Figures 1(b) and 1(c) represent the linkage diagrams in helicity basis with parallel linear (x,x) [or (y,y)] and cross-linear (x,y) [or (y,x)] polarized lights that are combinations of circular polarizations. Because of the symmetry between $|X_+\rangle$ and $|X_-\rangle$, the magnitudes of the transition probabilities are equal for the two paths $|O\rangle \leftrightarrow |X_+\rangle$ and $|O\rangle \leftrightarrow |X_-\rangle$, but the value is different, positive or negative. The positive (+) and negative (-) signs in Figs. 1(b) and 1(c) indicate the relative phases between the probability amplitudes of the transitions. In (x,x) [or (y,y)] polarizations, all transitions obtain a positive sign and then the closed loop introduces constructive interference and open the paths to the $|XX\rangle$ state. In (x,y) [or (y,x)] polarizations, the loop produces destructive interference and cannot generate biexcitons.

The three-state system is classified into three kinds of systems depending on the energy between the ground state and the other states: ladder, Λ , and V systems. The coherence of excitation into the two separate branches leads to several interesting effects in such a three-state system. In atomic systems, population trapping, quantum beats, and quantum jumps were observed in the three-state system.²³ The phenomena of quantum beats are also observed in the excitonic system in solid.

III. RESULTS AND DISCUSSION

A. Pump-probe experiment

Figure 2(a) shows the polarization-dependent transmission signals at 10 K in the 45-Å QW sample. The ratio between the pump and probe intensities is 1:0.22. The spin-polarized excitons with low kinetic energy can be generated in the $|X_+\rangle$ state by the σ_+ pump pulse according to the selection rule as shown in Fig. 1(a) and have a well-defined angular momentum because of the large hh-lh splitting (33 meV). In Fig. 2, (σ_+, σ_+) , (x,x) , and (x,y) indicate the light polarization combinations of the pump and probe pulses using the same definitions as in Fig. 1. The observed transmission decay in the (σ_+, σ_+) polarizations indicates the reduction of spin-polarized excitons in $|X_+\rangle$ by the phase-space-filling effect, while the transmission growth in the (σ_+, σ_-) polarizations indicates the accumulation of the opposite spin excitons in $|X_-\rangle$. These signals represent the dy-

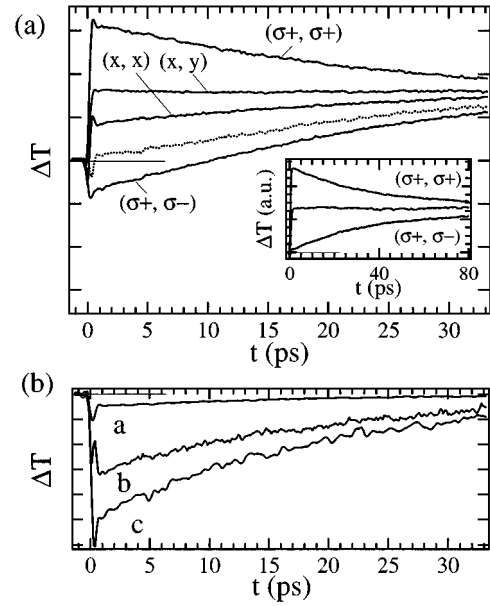


FIG. 2. Time evolution of the differential transmission signals at 10 K in the 45-Å QW's. (a) Spin-dependent component with a decay time of ~ 40 ps and the induced absorption due to biexciton formation (the pump-probe ratio is 1:0.22). The inset shows the time evolution of the signals at the lower probe intensity (the pump-probe ratio is 1:0.01). (b) Probe-intensity dependence of the induced absorption that corresponds to $(x,x) - (x,y)$. The pump-probe ratio is 1:0.03 (a), 1:0.22 (b), and 1:0.43 (c).

namical process of the exciton spin relaxation,^{4,24} which gives a new linkage between $|X_+\rangle$ and $|X_-\rangle$ states in Fig. 1.

The excitation by linearly polarized light generates the excitons in the $|X_+\rangle$ and $|X_-\rangle$ states with the same probabilities because of the symmetry between $|X_+\rangle$ and $|X_-\rangle$. Because the rates of the spin flip from $|X_+\rangle$ to $|X_-\rangle$ states and vice versa are equivalent, the signals in the (x,y) and (x,x) polarizations show spin-independent relaxation due to exciton recombination (a few nanoseconds) that is much longer compared to the spin relaxation time (~ 40 ps at 10 K).

According to the symmetry of the excitonic system and the selection rules, the transient behaviors of excitons in the $|X_+\rangle$ and $|X_-\rangle$ states should be symmetrical with respect to the signal level in linear polarizations and the (x,x) signal should be identical to the (x,y) signal if the upper transitions from exciton states to the biexciton state in Fig. 1 do not occur. But the measured signals are not symmetrical because the (σ_+, σ_-) signal shows a negative differential transmission (the induced absorption) in the initial picoseconds. The signal in the (x,x) polarizations similarly indicates induced absorption, deduced from the difference between the (x,y) and (x,x) signals. Note that the induced absorption occurs in only (σ_+, σ_-) and (x,x) polarizations according to the aforementioned selection rules. If the difference between the (x,y) and (x,x) signals adds to the (σ_+, σ_-) signal, the (σ_+, σ_-) signal changes to the time evolution (indicated by the dotted line) and the transient behaviors in the (σ_+, σ_+) and (σ_+, σ_-) polarizations become symmetrical precisely with respect to the signal level in the (x,y) polarizations. In fact, as shown in the inset, the time evolution indicates the

absence of induced absorption and symmetrical features for the probe intensities around $\frac{1}{100}$ of the pump intensity. The absence of population flow to the optically inactive exciton states with the angular momentum of ± 2 by the individual particle spin-flip of electron or hole is also ensured by the symmetrical properties of the (σ_+, σ_{\pm}) signals. The initial dip of the signal indicated by the dotted line represents that the (x, x) signal rises with a small time delay due to biexciton formation, while the (x, y) signal rises immediately.

Smith *et al.*³ observed the induced absorption in the pump-probe measurements of a 250-Å GaAs QW and discussed the biexcitonic contributions to the time-resolved pump-probe signals. They claim that the induced absorption due to biexciton formation was observed not in (x, x) polarizations but in (x, y) polarizations regardless of the biexciton formation by the optical transition, but not by the collision. Additionally, their results do not indicate the symmetrical transient behaviors, and the symmetries of the system and selection rule are broken. We consider that their results are affected by the biexciton formation due to the collision between excitons.

Increasing the probe intensity, the induced absorption increases as shown in Fig. 2(b). The induced absorption represents the instantaneous biexciton formation by the absorption of the probe pulse and the dissociation of biexcitons with the time constant of ~ 20 ps. Simultaneously, spin-polarized excitons that are generated initially in the $|X_+\rangle$ state by the σ_+ polarized pump pulse flip their spins by the exchange interaction and go into the $|X_-\rangle$ state with the time constant of ~ 40 ps.²⁴ The biexciton dissociation time is not sensitive to the probe intensity in the observed intensity range 1:0.03–1:0.5. The similar induced absorption and symmetrical properties of the signals were observed in the other samples in the reflection geometric pump-probe experiments.

As a result of the pump-probe experiments, we could observe the biexciton formation and clearly show the polarization selection rule of the exciton-biexciton system. The detailed results related to the spin relaxation and biexcitonic contributions at low temperatures will be reported elsewhere.

B. Four-wave-mixing experiment

Figure 3(a) shows the FWM signals in the 150-Å QW's for four specific polarization combinations between the pump and probe pulses. The excitation energy is fixed at 1.532 eV, which is detuned by 5 meV to the lower-energy side from the hh exciton resonance. The strong oscillatory behavior is seen in the (x, x) and (σ_+, σ_-) polarizations, while no oscillatory behavior is observed in the (σ_+, σ_+) polarizations and the weak modulation in the (x, y) polarizations. All the FWM signals are normalized to their maximum value. We could obtain the oscillatory signals over the entire sample and the origin of the oscillation is assumed to be intrinsic, such as biexcitons. If the origin of the oscillation is extrinsic, such as bound excitons, one may or may not observe the oscillatory signals depending on the illuminated position in the sample. The photoluminescence (PL) spectrum at 10 K in the inset of Fig. 3(a) shows a free hh exciton peak (dashed line) at 1.537 eV, with no measurable Stokes shift, and a tailed lower-energy component (dotted line) that reveals superlinear growth against the excitation intensity,

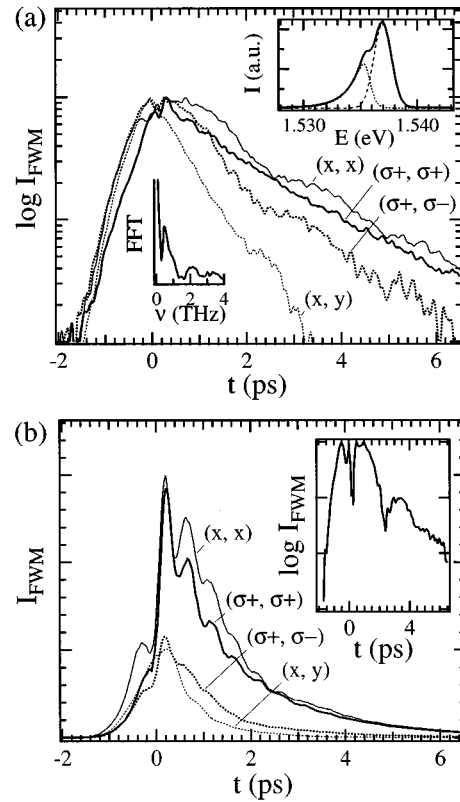


FIG. 3. (a) Semilog plot of the FWM signals in four specific polarizations of the pump and probe pulses at 10 K in 150-Å QW's. The excitation energy is ~ 1.532 eV. All the signals are normalized to their maximum value. The upper inset shows the PL spectrum at 10 K. The lower inset shows the power spectrum of the difference signal $(x, x) - (\sigma_+, \sigma_+)$. The two peaks correspond to the frequencies of the exciton-biexciton quantum beats (~ 0.43 THz) and hh-lh quantum beats (~ 2.05 THz), respectively. (b) FWM signals in the excitation energy of 1.538 eV show the hh-lh quantum beats. The inset shows the semilog plot of the difference $(x, x) - (\sigma_+, \sigma_+)$ that still represents the exciton-biexciton quantum beats.

while the exciton PL component reveals linear growth. The tailed lower-energy component is fitted well by the inverse Boltzmann function, which is used frequently for biexciton distribution.¹ But the superlinear growth is not necessarily indicative of biexciton formation according to the elaborate work by Osborne *et al.*²¹ If the origin of the beat is the charged-exciton-bound (or free) -exciton beat, the beat appears in (σ_+, σ_+) , but not in (σ_+, σ_-) , because the system becomes the assembly of two-level systems.

We consider here the excitonic contribution and the biexcitonic contribution to the FWM signal due to the single-photon absorption from the pump and probe pulses. According to the transition selection rules shown in Fig. 1, the FWM signals in the (σ_+, σ_+) and (σ_+, σ_-) polarizations originate from the excitonic and the biexcitonic components, respectively, and the signal (x, x) includes both contributions. Therefore, the clear oscillatory signals in the (x, x) and (σ_+, σ_-) polarizations are considered as the exciton-biexciton quantum beats. The signal in the (x, y) polarizations should not generate any signal according to the transition selection rule except for two-photon absorption; in fact, the signal is more than one order of magnitude weaker than

those in the (x,y) and $(\sigma+, \sigma+)$ polarizations. Numerous measurements have reported anomalous FWM signals in the (x,y) polarizations and various models have been proposed so far, but none of them consistently described the feature. The treatment of the (x,y) polarizations has not been established yet and is beyond the scope of this paper because of its lack of influence on our discussion.

The beat period is approximately 2.3 ps and the Fourier transformation of $(\sigma+, \sigma-)$ shows a peak at 1.8 meV that coincides well with the peak separation of 1.7 meV in the PL spectrum. Leo *et al.*²⁵ observed the beating between free and bound excitons with a period of 2.8 ps (~ 1.5 meV) in 170-Å GaAs MQW's. The value 1.8 meV may be easily recognized as the binding energy of excitons bound to impurities in QW's. But the beating between free and bound excitons appears in (x,x) and $(\sigma+, \sigma+)$, but not in $(\sigma+, \sigma-)$ polarizations. The biexciton formation is also confirmed at the same pump intensity as the induced absorption in the pump-probe measurement. The power dependence of the beating amplitude also supports that this beating is the quantum beats between the biexciton and exciton since the beating amplitude of the free-exciton-bound-exciton beats decreases rapidly with increasing laser power due to the bound exciton saturation effect.

As a result, the exciton-biexciton quantum beats and the beating between free excitons and bound excitons can be distinguished by the polarization dependence of the FWM signals. The experimental distinction between the polarization interference and the quantum beats are demonstrated using the time-resolved FWM by Koch *et al.*²⁶ and the spectrally resolved time-integrated FWM by Lyssenko *et al.*²⁷ These methods are very useful and can be applied to more general cases, although they are more complicated than the method using the polarization dependence of time-integrated FWM signals demonstrated here.

Another oscillatory time dependence with a different period was also observed at the excitation energy of 1.538 eV [Fig. 3(b)]. The beating was observed in all polarization combinations. The beating period is 490 fs, which corresponds to 8.5 meV. The energy 8.5 meV agrees very well with the splitting energy 8.4 meV between the hh and lh exciton transitions in the PL excitation spectrum. Therefore this rapid beating is considered as the well-known quantum beats between the hh and lh excitons.²⁸ The quantum beats occur when two states are excited simultaneously and connects through the common state in the V system. The laser has a spectral bandwidth of 12 meV (FWHM) and can excite the hh and lh excitons simultaneously. All characteristic features of the hh-lh quantum beats, such as the appearance in all polarizations, a 90° phase shift between the (x,x) and (x,y) signals, and the beating in the negative delay, are clearly observed.

Surprisingly, the biexcitonic contribution is still extracted from the signals in Fig. 3(b) by having the difference between the (x,x) and $(\sigma+, \sigma+)$ signals. The inset of Fig. 3(b) shows the difference $(x,x) - (\sigma+, \sigma+)$, which indicates the biexcitonic contribution because the signal $(\sigma+, \sigma+)$ originates from the excitonic component and the (x,x) originates from the excitonic and biexcitonic components. The beating period precisely coincides with that in Fig. 3(a). Increasing the excitation energy to the lh exciton

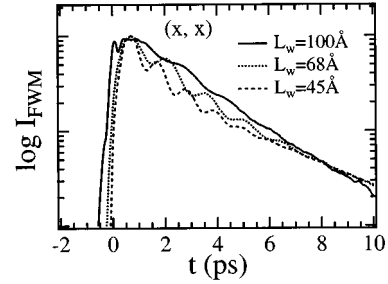


FIG. 4. FWM signals in (x,x) polarizations in the hh exciton resonant excitation in the samples with a well thickness of 100 Å (solid line), 68 Å (dotted line), and 45 Å (dashed line).

transition, the beating increasingly consists of only the hh-lh quantum beats. The weak influence of the hh-lh quantum beats is also found in the signals of Fig. 3(a), which appears as a small second peak around 2 THz in the power spectrum [inset of Fig. 3(a)].

Figure 4 shows the beating FWM signals in the (x,x) polarizations for the QW's with a well width of 100, 68, and 45 Å. All the signals are normalized to their maximum value. The similar polarization dependence of the exciton-biexciton quantum beats in the 150-Å QW's are also observed in each sample. The biexciton binding energies can be deduced from the beating period of the difference $(x,x) - (\sigma+, \sigma+)$ and are 2.4, 2.8, and 3.5 meV in the samples with a well width of 100, 68, and 45 Å, respectively.

The observed well-width dependence of the biexciton binding energy can be compared with the previous works. Figure 5 shows the observed biexciton binding energies (E_b^{xx}) in the type-I QW's with different well widths, as shown in Fig. 5 (see the quoted references about the details of each work). Although E_b^{xx} should be plotted versus the strength of quantum confinement, this figure gives a measure of the magnitude of E_b^{xx} versus the well width. The open

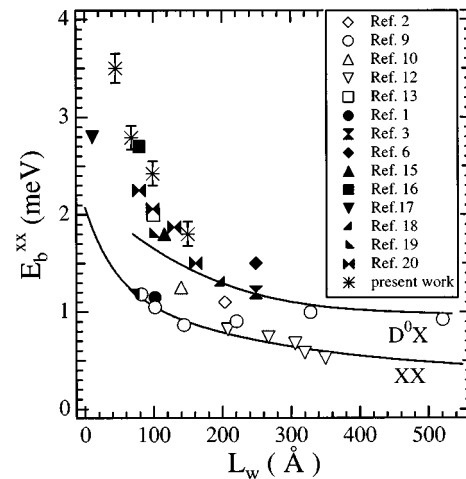


FIG. 5. hh biexciton binding energy in the type-I GaAs QW's versus the well thickness. The open and solid marks are the experimental values. The upper and lower solid lines are the theoretical results for the donor at the center of the well (D^0X) and biexciton (XX) binding by Kleinman. See the quoted references about the details of each work.

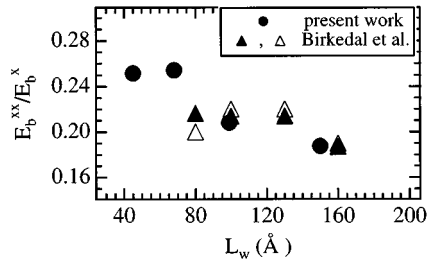


FIG. 6. Ratio E_b^{xx}/E_b^x between the biexciton and exciton binding energies versus the well thickness L_w .

marks (diamond, circles, triangle, inverted triangles, and square) are the experimental results by the cw PL measurement and the line-shape analysis. The solid marks are the values determined by the quantum beats in the FWM experiments. The lower solid line (XX) indicates the theoretical prediction for E_b^{xx} by Kleinman⁸ using the six-parameter variational wave function. The upper solid line (D_0X) is also the calculated result⁸ for the binding energy of exciton bound to a donor at the center of the well.

The values obtained in our present work are also plotted by the error bars in Fig. 5. The binding energies in the 150-, 100-, and 68-Å QW's are found to be adequate values compared with previous works where the binding energy is deduced by the FWM technique, and the value 3.5 meV in 45-Å QW's is the largest, to the authors' knowledge, reported so far. Most experimental values, including our results, indicate the larger binding energies that match for D_0X rather than for XX, and the prediction for biexcitons by Kleinman seems to give the lower limit of E_b^{xx} . The explanation for the discrepancy between theory and experiment has not been given yet. Recently, Birkedal *et al.*²⁰ performed the systematic experimental study of the well-width dependence of E_b^{xx} for a range of well thickness 80–160 Å and conclude that the ratio of the biexciton and exciton binding energies E_b^{xx}/E_b^x is independent of the well width having a value of approximately 0.23.

The ratio E_b^{xx}/E_b^x obtained in our experiments is shown in Fig. 6. In Fig. 6 the results by Birkedal *et al.* are indicated by open triangles. The solid triangles indicate the ratio between the observed E_b^{xx} by Birkedal *et al.* and our calculated E_b^x . The exciton binding energy E_b^x , which is listed in Table I, is calculated by the accurate theory²² including valence-band mixing, nonparabolicity of the bulk conduction band, Coulomb coupling between excitons belonging to different subbands, and the difference in dielectric constants between well and barrier materials. The hh-lh splitting energies calculated by that theory coincide well with the observed values in our samples and we suppose that the exciton binding energy E_b^x can be estimated correctly by the theoretical calculation. The ratio E_b^{xx}/E_b^x is much larger than that by Kleinman⁸ (~ 0.13) and gradually increases with decreasing well width. As a result, our experimental results also imply that the current theoretical prediction underestimates the biexciton binding energy, but we doubt the well-width independence of the ratio E_b^{xx}/E_b^x by our measurements in a broader range of the well width (45–150 Å) than that of Birkedal *et al.*

IV. CONCLUSION

In summary, we clearly demonstrated the useful and convenient distinction between exciton-biexciton quantum beats and other beats using the polarization dependence of the time-integrated FWM signals. The biexciton creation should be confirmed by the polarization dependence of the beat signals instead of the power dependence of the emission spectrum. The quantum beats between the exciton and biexciton in the FWM signals are observed and the well-width dependence of the biexciton binding energy is shown in the range of the well width 45–150 Å. We observed a larger binding energy in the 45-Å QW sample than that reported so far and confirmed the biexciton formation using the polarization dependence in the FWM and pump-probe signals. Recently, biexcitons with a binding energy of 3 meV in the (GaAs)₁₂(AlAs)₁₂ *type-II* superlattices were also observed,²⁹ a unified theoretical picture is earnestly desired.

*Present address: Massachusetts Institute of Technology, Department of Chemistry, Cambridge, MA 02139.

¹D. J. Lovering, R. T. Phillips, G. J. Denton, and G. W. Smith, Phys. Rev. Lett. **68**, 1880 (1992).

²R. T. Phillips, D. J. Lovering, G. J. Denton, and G. W. Smith, Phys. Rev. B **45**, 4308 (1992).

³G. O. Smith, E. J. Mayer, J. Kuhl, and K. Ploog, Solid State Commun. **92**, 325 (1994).

⁴S. Adachi, S. Takeyama, Y. Takagi, A. Tackeuchi, and S. Muto, Appl. Phys. Lett. **68**, 964 (1996).

⁵S. Adachi and Y. Takagi, Solid State Commun. (to be published).

⁶K. Bott, O. Heller, D. Bennhardt, S. T. Cundiff, P. Thomas, E. J. Mayer, G. O. Smith, R. Eccleston, J. Kuhl, and K. Ploog, Phys. Rev. B **48**, 17 418 (1993).

⁷G. Finkelstein, S. Bar-Ad, O. Carmel, I. Bar-Joseph, and Y. Levinson, Phys. Rev. B **47**, 12 964 (1993).

⁸D. A. Kleinman, Phys. Rev. B **28**, 871 (1983).

⁹R. C. Miller, D. A. Kleinman, A. C. Gossard, and O. Munteanu, Phys. Rev. B **25**, 6545 (1982).

¹⁰S. Charbonneau, T. Steiner, M. L. W. Thewalt, Emil S. Koteles, J. Y. Chi, and B. Elman, Phys. Rev. B **38**, 3583 (1988).

¹¹R. Cingolani, Y. Chen, and K. Ploog, Phys. Rev. B **38**, 13 478 (1988).

¹²D. C. Reynolds, K. K. Bajaj, C. E. Stutz, R. J. Jones, W. M. Theis, P. W. Yu, and K. R. Evans, Phys. Rev. B **40**, 3340 (1989).

¹³R. Cingolani, K. Ploog, G. Peter, R. Hahn, E. O. Göbel, C. Moro, and A. Cingolani, Phys. Rev. B **41**, 3272 (1990).

¹⁴B. F. Feuerbacher, J. Kuhl, and K. Ploog, Phys. Rev. B **43**, 2439 (1991).

¹⁵K. -H. Pantke, D. Oberhauser, V. G. Lyssenko, J. M. Hvam, and G. Weimann, Phys. Rev. B **47**, 2413 (1993).

¹⁶S. Bar-Ad and I. Bar-Joseph, Phys. Rev. Lett. **68**, 349 (1992).

¹⁷H. H. Yaffe, Y. Prior, J. P. Harbison, and L. T. Florez, J. Opt. Soc. Am B **10**, 578 (1993).

¹⁸E. J. Mayer, G. O. Smith, V. Heuckeroth, J. Kuhl, K. Bott, A. Schulze, T. Meier, D. Bennhardt, S. W. Koch, P. Thomas, R. Hey, and K. Ploog, Phys. Rev. B **50**, 14 730 (1994).

- ¹⁹J. C. Kim, D. R. Wake, and J. P. Wolfe, *Phys. Rev. B* **50**, 15 099 (1994).
- ²⁰D. Birkedal, J. Singh, V. G. Lyssenko, J. Erland, and J. M. Hvam, *Phys. Rev. Lett.* **76**, 672 (1996).
- ²¹J. L. Osborne, A. J. Shields, M. Pepper, F. M. Bolton, and D. A. Ritchie, *Phys. Rev. B* **53**, 13 002 (1996).
- ²²L. C. Andreani and A. Pasquarello, *Phys. Rev. B* **42**, 8928 (1990).
- ²³S. B. W. Shore, in *The Theory of Coherent Atomic Excitation* (Wiley, New York, 1990), Vols. 1 and 2.
- ²⁴S. Adachi, S. Takeyama, Y. Takagi, and A. Tackeuchi (unpublished).
- ²⁵K. Leo, T. C. Damen, J. Shah, and K. Kohler, *Phys. Rev. B* **42**, 11 359 (1990).
- ²⁶M. Koch, J. Feldmann, G. von Plessen, E. O. Göbel, P. Thomas, and K. Köhler, *Phys. Rev. Lett.* **69**, 3631 (1992).
- ²⁷V. G. Lyssenko, J. Erland, I. Balslev, K.-H. Pantke, B. S. Razbirin, and J. M. Hvam, *Phys. Rev. B* **48**, 5720 (1993).
- ²⁸K. Leo, T. C. Damen, J. Shah, E. O. Göbel, and K. Köhler, *Appl. Phys. Lett.* **57**, 19 (1990).
- ²⁹M. Nakayama, K. Suyama, and H. Nishimura, *Phys. Rev. B* **51**, 7870 (1995).